

structure, which probably means that at least some of the truncated tetrahedral sites are occupied by larger A^+ ions in order for the structure to form.

The modified pyrochlore and tetragonal tungsten bronze structures demonstrate how physical properties depend on structure. The most striking difference between the magnetic properties of the two structures (Table I) is the large negative Θ values of the modified pyrochlores as opposed to mostly small positive Θ values for the tetragonal bronze compounds. This difference is a consequence of the relative number of $M^{2+}-F^- - M^{2+}$, $M^{3+}-F^- - M^{3+}$, and $M^{2+}-F^- - M^{3+}$ near-neighbor interactions, which is 1:1:2 in the cubic, modified pyrochlore structure and 1:1:13 in the ordered, tetragonal bronze structure. It is because of the relatively large number of $M^{2+}-F^- - M^{3+}$ near-neighbor interactions (which are ferromagnetic) that the Θ values of the tetragonal bronze compounds are positive.

It is not surprising that long-range magnetic ordering was not observed in the modified pyrochlore phases since this structure gives rise to so many magnetic constraints (frustrations). Differences in the magnetic properties of $K_{0.50}Ni_{0.50}Cr_{0.50}F_3$ and $K_{0.50}Ni_{0.50}V_{0.50}F_3$, however, are surprising. From Figure 6, it appears that a considerable amount of magnetic coupling occurs in (Ni,V) near 100 K. We assume this is antiferromagnetic coupling between neighboring Ni^{2+} ions. What is strange is that no such effect is seen in (Ni,Cr). One possible explanation is that

(Ni,V) goes through some crystallographic phase change between 100 and 300 K.

Conclusions

The most important conclusion of this work is that $M^{2+}-M^{3+}$ ionic ordering is common in first-row transition metal fluorides having the tetragonal tungsten bronze structure. In $K_xMn_xCr_{1-x}F_3$, $K_xMn_xV_{1-x}F_3$, $K_{0.60}Ni_{0.60}Cr_{0.40}F_3$, and $Na_{0.25}K_{0.25}Mn_{0.50}Cr_{0.50}F_3$ $|J_{2+,2+}| \approx |J_{3+,3+}| \gg |J_{2+,3+}|$. This difference in magnitude of magnetic coupling energies causes magnetic ordering to occur in steps. Although neutron diffraction studies are necessary to unambiguously confirm the magnetic structures, it appears that linear trimers form first, giving rise to a quasi-paramagnetic region, followed by long-range magnetic ordering at a lower temperature. The 180° $M^{2+}-F^- - M^{3+}$ interactions ($M^{2+} = Mn, Ni; M^{3+} = V, Cr$) are ferromagnetic. The modified pyrochlore structure sometimes forms with smaller alkali metal ions like K^+ and Na^+ . At some compositions, these compounds form ordered structures of lower symmetry, although they remain cubic.

Acknowledgment. We gratefully acknowledge the National Science Foundation (Grants DMR 79-00313, DMR 76-83360, and DMR 77-11970) for financial support, including the purchase of major equipment, and The University of Mississippi for cost sharing. Appreciation is expressed to The University of Mississippi Computer Center for providing data reduction time.

Contribution from the Departamento de Química Inorgánica, Facultad de Ciencias, Universidad de Málaga, 29071 Málaga, Spain, and Department of Chemistry, University of Cambridge, Lensfield Road, Cambridge CB2 1EW, U.K.

Order and Disorder of Vanadyl Chains: Crystal Structures of Vanadyl Dihydrogen Arsenate $(VO(H_2AsO_4)_2)$ and the Lithium Derivative $Li_4VO(AsO_4)_2$

Miguel A. G. Aranda,[†] J. Paul Attfield,[‡] Sebastian Bruque,^{*,†} and Maria Martinez-Lara[†]

Received July 10, 1991

The crystal structure of layered, tetragonal $VO(H_2AsO_4)_2$ ($a = 9.1305$ (1) Å, $c = 8.1318$ (2) Å) has been refined in space group $I4/mcm$ from laboratory X-ray powder diffraction data by the Rietveld method, giving $R_{wp} = 10.1\%$ and $R_F = 5.5\%$. Disorder of the vanadium atoms over two sites results from infinite $\cdot V=O \cdots V=O \cdot$ chains orienting in the $\pm c$ -directions at random, due to the flexibility of the arsenate groups that link neighboring chains. The two modes of ordering the vanadyl chains to give structures with $P4/ncc$ and $I4cm$ symmetry, both of which have been reported, are also discussed. The structure of the lithium derivative $Li_4VO(AsO_4)_2$ ($a = 9.0293$ (2) Å, $c = 9.0053$ (4) Å), obtained by ion exchange, has $P4/ncc$ symmetry due to partial ordering between vanadyl chains and has been refined to $R_{wp} = 13.8\%$ and $R_F = 9.3\%$. The lithium ions occupy irregular five-coordinate sites between vanadyl arsenate layers. The different behavior of the $VO(H_2XO_4)_2$ compounds ($X = P, As$) toward ionic exchange reactions is discussed in the light of these results.

Introduction

Vanadium phosphorus oxides have a rich and complex structural chemistry owing to the variable oxidation state of vanadium and the variety of observable phosphorus to vanadium ratios. These compounds have been extensively studied due to their interesting catalytic properties¹⁻³ and their ability to act as host materials for ion exchange and intercalation reactions.^{4,5} Butane and butene can be oxidized to maleic anhydride with air over vanadium phosphate catalysts.^{6,7} The consensus of the studies is that the best catalysts have vanadium in the +4 oxidation state and a P/V ratio of approximately 1 and $(VO)_2P_2O_7$, which exhibits these values, has been detected in active catalysts with high selectivities.

Although vanadium phosphates have been widely studied,⁸ possible arsenic analogues have received less attention. We have recently reported the synthesis and characterization of vanadyl dihydrogen arsenate $VO(H_2AsO_4)_2$ and the lithium derivative $Li_4VO(AsO_4)_2$ obtained by a "chimie douce" reaction.⁹ The crystal structure of the apparently isostructural vanadyl dihydrogen phosphate, $VO(H_2PO_4)_2$, has been reported,¹⁰ but according to

the literature this compound does not exchange H^+ with Li^+ or other cations.¹¹ We have therefore investigated the structures of $VO(H_2AsO_4)_2$ and $Li_4VO(AsO_4)_2$ to clarify the differences between the crystal chemistries and ion-exchange reactions of the arsenate and phosphate compounds.

Experimental Section

The synthesis and chemical analysis of $VO(H_2AsO_4)_2$ and $Li_4VO(AsO_4)_2$ were carried out as described elsewhere.⁹ Both preparations

- (1) Bordes, E.; Courtine, P. *J. Catal.* **1979**, *57*, 236.
- (2) Hodnett, B. K.; Delmon, B. *Appl. Catal.* **1983**, *6*, 245.
- (3) Poli, G.; Resta, I.; Ruggeri, O.; Trifiro, F. *Appl. Catal.* **1981**, *1*, 375.
- (4) Martinez-Lara, M.; Jimenez-Lopez, A.; Moreno-Real, L.; Bruque, S.; Casal, B.; Ruiz-Hitzky, E. *Mater. Res. Bull.* **1988**, *20*, 549.
- (5) Ladwig, G. Z. *Anorg. Allg. Chem.* **1965**, *338*, 266.
- (6) Hodnett, B. K.; Permann, P.; Delmon, B. *Appl. Catal.* **1983**, *6*, 231.
- (7) Vartuli, J. C.; Zener, J. R.; U.S. Patent 4247 419, 1981.
- (8) Beltran-Porter, D.; Beltran-Porter, A.; Amoros, P.; Ibanez, R.; Martinez, E.; Le Bail, A.; Ferey, C.; Villeneuve, G. *Eur. J. Solid State Inorg. Chem.* **1991**, *28*, 131.
- (9) Martinez-Lara, M.; Bruque, S.; Moreno, L.; Aranda, M. A. G. *J. Solid State Chem.* **1991**, *91*, 25.
- (10) Linde, S. A.; Gorbunova, Y. E.; Lavrov, A. V.; Kuznetsov, V. G. *Dokl. Akad. Nauk SSSR* **1979**, *244*, 1411.
- (11) Ladwig, G. Z. *Chem.* **1968**, *8*, 307.

[†] Universidad de Málaga.
[‡] University of Cambridge.

Table I. Profile and Structural Parameters from the Refinement of $\text{VO}(\text{H}_2\text{AsO}_4)_2$ in Space Group $I4/mcm$ (No. 140), with Esd's in Parentheses

Cell Dimensions (Å)						
$a = 9.1305$ (1)					$c = 8.1318$ (2)	
Data						
no. of reflns = 345		no. of points = 2900		no. of refined params = 26		
R Factors (%)						
$R_{wp} = 10.1$		$R_p = 7.1$		$R_F = 5.5$		
Atomic Parameters ^a						
atom	sym position	x	y	z	isotrop B-factor, Å ²	site occ
V	8f	1/4	1/4	0.1979 (4)	0.4 (1)	0.5
As	8h	-0.0341 (1)	0.0341	1/4	0.73 (3)	1.0
O(1)	16k	0.1456 (5)	0.0662 (5)	1/4	1.6 (1)	1.0
O(2)	16l	0.8871 (4)	0.1129	0.0838 (6)	1.5 (1)	1.0
O(3)	4a	1/4	1/4	0	1.2 (3)	1.0
H	16l	0.147 (3)	-0.147	0.484 (6)	4	1.0

^a For the sake of consistency with the parameters of $\text{VO}(\text{H}_2\text{PO}_4)_2$ and $\text{Li}_4\text{VO}(\text{AsO}_4)_2$, the coordinates are given relative to the origin of space group $P4/ncc$ (No. 130). Coordinates in the standard setting of $I4/mcm$ may be obtained by subtracting $(1/4, 1/4, 1/4)$ from the above values.

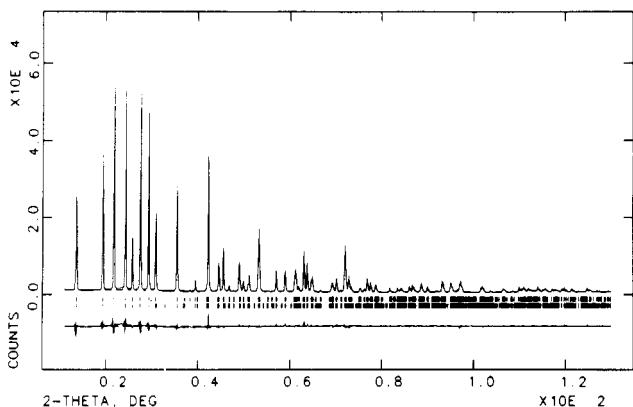


Figure 1. Final observed (points), calculated (full line), and difference X-ray diffraction profiles for $\text{VO}(\text{H}_2\text{AsO}_4)_2$. Reflection bars are calculated for $I4/mcm$ (upper) and $P4/ncc$ (lower) symmetries.

were performed in ethanol at atmospheric pressure and temperatures below 79 °C.

Powder X-ray diffraction profiles of the two arsenates were recorded on a Siemens D501 automated diffractometer using graphite-monochromated $\text{Cu K}\alpha$ radiation. The powder pattern for $\text{VO}(\text{H}_2\text{AsO}_4)_2$ was recorded between 14 and 130° in 2θ , in 0.04° steps, counting for 20 s per point, and for $\text{Li}_4\text{VO}(\text{AsO}_4)_2$, the pattern was scanned in steps of 0.03° over the angular range 14–120° in 2θ counting for 15 s per step. Rietveld refinements¹² were performed with the GSAS program¹³ using a pseudo-Voigt peak shape function, corrected for asymmetry at low angles, and a refined background function.

Results

$\text{VO}(\text{H}_2\text{AsO}_4)_2$. The powder pattern of this compound was indexed with the TREOR program¹⁴ on a tetragonal cell with dimensions $a = 9.128$ (1) Å and $c = 8.128$ (1) Å.⁹ This cell is very similar to that of $\text{VO}(\text{H}_2\text{PO}_4)_2$ ($a = 8.953$ Å, $c = 7.965$ Å),¹⁰ and so the profile was fitted using the latter structure, which has $P4/ncc$ symmetry, as the starting model. The Rietveld refinement of the VAs_2O_9 framework converged successfully giving $R_{wp} = 12.7\%$, but a large isotropic temperature factor of 2.9 (1) Å² was obtained for the vanadium atom. Refining this atom anisotropically gave a large value for U_{33} , showing that V is disordered in the c -direction.

A careful examination of the powder pattern of $\text{VO}(\text{H}_2\text{AsO}_4)_2$ revealed that reflections with odd values of $(h + k + l)$ were absent (see Figure 1), showing that the space group symmetry is in fact $I4/mcm$. This higher symmetry corresponds to the introduction of a mirror plane into the $P4/ncc$ group at $z = 1/4$. Although this doubles the number of general symmetry positions, all of the atoms

Table II. Bond Distances (Å) and Angles (deg) for $\text{VO}(\text{H}_2\text{AsO}_4)_2$, with Esd's in Parentheses

V-O(1) (×4)	1.976 (4)	As-O(2) (×2)	1.692 (4)
V-O(3)	1.610 (3)	O(2)-H	0.91 (4)
V-O(3')	2.456 (3)	O(2)···H' (×2)	2.29 (2)
As-O(1) (×2)	1.666 (4)		
O(1)-V-O(1')	87.37 (4)	O(1)-As-O(2)	110.1 (1)
O(1)-V-O(1'')	155.3 (2)	O(2)-As-O(2)'	106.0 (3)
O(1)-V-O(3)	102.4 (1)	V-O(1)-As	128.6 (3)
O(1)-V-O(3')	77.6 (1)	As-O(2)-H	172 (3)
O(3)-V-O(3')	180	As-O(2)···H	132 (1)
O(1)-As-O(1)'	110.3 (3)	O(2)-H···O(2)'	120 (2)

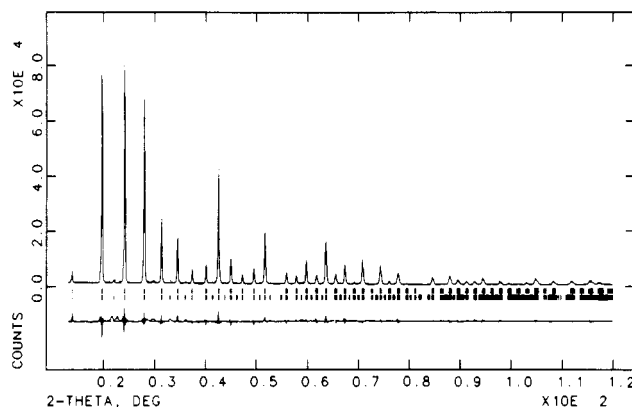


Figure 2. Final observed (points), calculated (full line), and difference X-ray profiles for $\text{Li}_4\text{VO}(\text{AsO}_4)_2$ with reflection bars as in Figure 1.

in the As_2O_9 framework were found to lie on fully occupied special positions in the higher space group, and only V is disordered over the two available sites at $(1/4, 1/4, 1/4 \pm z)$. Refinement of the $I4/mcm$ model gave a good profile fit with $R_{wp} = 10.4\%$ and $R_F = 5.9\%$. Finally the position of the hydrogen atom was also refined in the $(x, -x, z)$ plane by restraining the O-H bond distance. This improved the fit slightly to $R_{wp} = 10.1\%$ and $R_F = 5.5\%$, giving the results shown in Tables I and II. The final observed, calculated, and difference profiles are shown in Figure 1.

$\text{Li}_4\text{VO}(\text{AsO}_4)_2$. The diffraction pattern was indexed on the previously reported cubic unit cell with $a = 9.025$ Å,⁹ except for two very weak impurity peaks which did not hamper the subsequent refinement. As the layered $\text{VO}(\text{H}_2\text{AsO}_4)_2$ structure cannot be described in a cubic space group, we assumed that the structure of $\text{Li}_4\text{VO}(\text{AsO}_4)_2$ is also tetragonal, with an accidental degeneracy of a and c . Weak peaks with odd values of $(h + k + l)$ were observed (Figure 2), and so the structure was refined in space group $P4/ncc$ using the coordinates determined for $\text{VO}(\text{H}_2\text{AsO}_4)_2$ as a starting model. Refinement of an ordered VAs_2O_9 framework converged to $R_{wp} = 16.6\%$ and $R_F = 11.5\%$, and again a very high isotropic temperature factor for the vanadium atom (4.4 (3) Å²)

(12) Rietveld, H. M. *J. Appl. Crystallogr.* **1969**, *2*, 65.

(13) Larson, A. C.; Von Dreele, R. B. Los Alamos National Laboratory Report No. LA-UR-86-748, 1987.

(14) Werner, P. E. *Z. Kristallogr.* **1969**, *120*, 375.

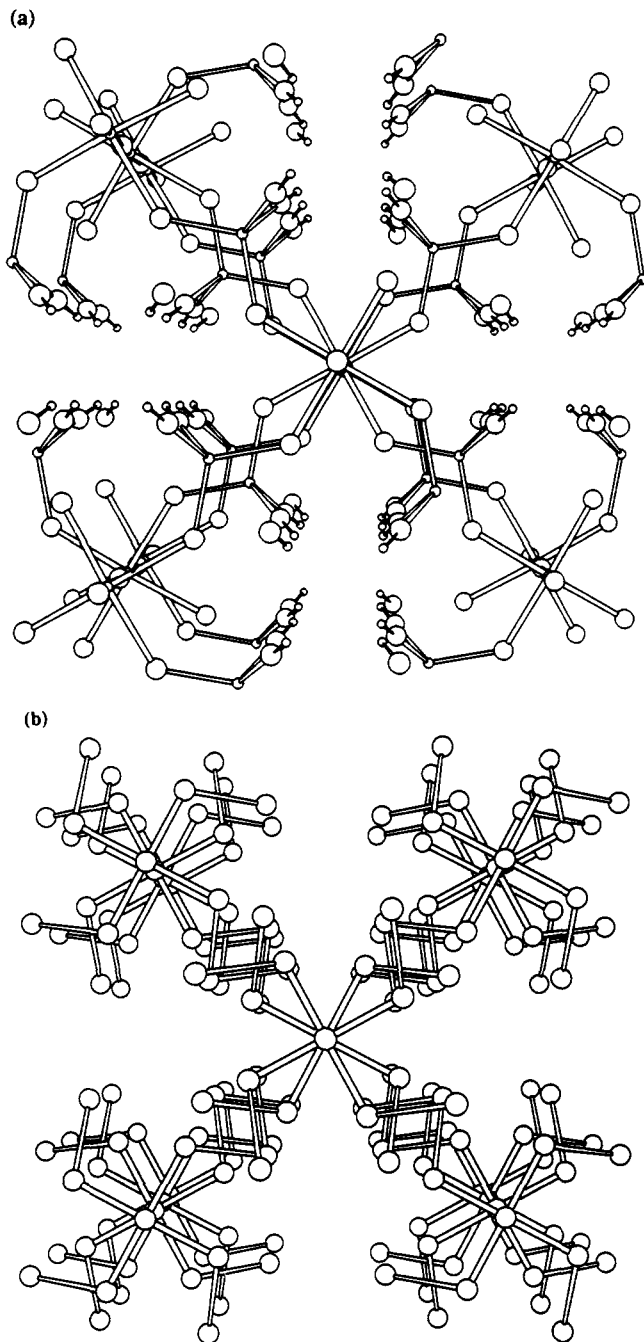


Figure 3. Perspective views along the c axis of (a) $\text{VO}(\text{H}_2\text{AsO}_4)_2$ and (b) Bi_2CuO_4 .

showed that this atom is disordered, as occurs in $\text{VO}(\text{H}_2\text{AsO}_4)_2$. With vanadium disordered over two sites, the refinement was improved to $R_{\text{wp}} = 14.8\%$ and $R_F = 9.5\%$. The Fourier difference map revealed a peak at $(0.10, -0.17, 0.09)$ that was assigned to the lithium atom, but no evidence for any H_2O between the layers. Final refinement of all the atoms, with restraints on the Li-O bond distances, gave $R_{\text{wp}} = 13.8\%$ and $R_F = 9.3\%$ and the results in Tables III and IV. Final observed, calculated, and difference profiles are displayed in Figure 2.

Discussion

Views of the layered structure of $\text{VO}(\text{H}_2\text{AsO}_4)_2$ are shown in Figures 3a and 4. Each layer consists of vanadyl groups linked to four neighboring groups by near-regular arsenate tetrahedra. Each arsenate group links two vanadyl units, and the remaining two arsenate oxygens are protonated. Successive layers are held together by $\text{VO}\cdots\text{VO}$ interactions and hydrogen bonding between a protonated oxygen from one layer and two protons in the next, as shown in Figure 4. The hydrogen position differs slightly from

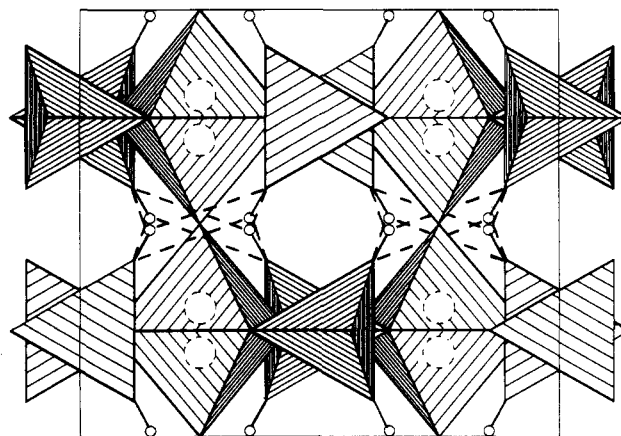


Figure 4. (010) polyhedral view (c vertical) of $\text{VO}(\text{H}_2\text{AsO}_4)_2$ with the 50% occupied vanadium sites shown as broken circles. The hydrogen atoms are shown as small circles with O-H and O \cdots H bonds as continuous and broken lines, respectively.

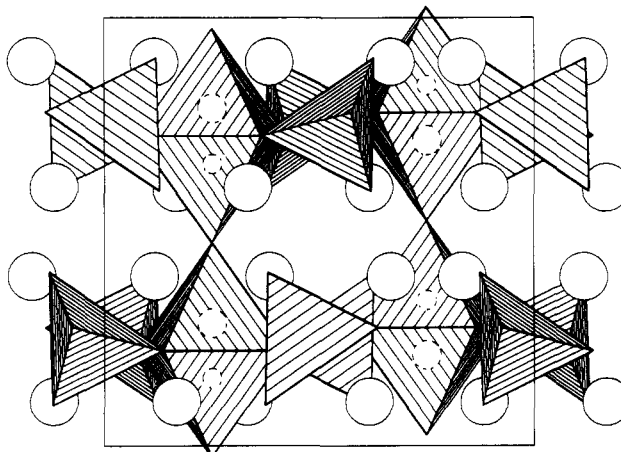


Figure 5. (010) polyhedral view (c vertical) of $\text{Li}_4\text{VO}(\text{AsO}_4)_2$ with the 65% and 35% occupied vanadium sites shown as large and small broken circles, respectively, and lithiums shown as full circles.

that reported in $\text{VO}(\text{H}_2\text{PO}_4)_2$;¹⁰ a neutron study will be performed to address this problem. This stacking of layers results in infinite vanadyl chains parallel to c at $(\frac{1}{4}, \frac{1}{4}, z)$, with octahedral coordination around V, and also forms channels in the same direction (Figure 4) around $(\frac{1}{4}, \frac{3}{4}, z)$ in which the hydrogens reside. V is bonded to four equatorial arsenate oxygens at distances of 1.98 Å and to the two axial oxygens with a short V=O bond of 1.61 Å and a long V \cdots O interaction of 2.46 Å.

The structure of $\text{VO}(\text{H}_2\text{AsO}_4)_2$ differs from that of $\text{VO}(\text{H}_2\text{P}_2\text{O}_7)_2$ ¹⁰ in that the vanadiums are disordered over the two available sites within each octahedron, as shown in Figure 3, which results in a crystallographic mirror plane at $z = \frac{1}{4}$ and raises the space group symmetry from $P4/ncc$ to $I4/mcm$. Another powder X-ray study of $\text{VO}(\text{H}_2\text{AsO}_4)_2$ reported during the course of this work also found disorder of the vanadiums but did not consider the possibility of $I4/mcm$ symmetry.¹⁵ However, a very recent structure determination using a $\text{VO}(\text{H}_2\text{AsO}_4)_2$ crystal prepared under hydrothermal pressure found cell parameters $a = 9.131(1)$ Å and $c = 8.146(3)$ Å, and systematic absences that correspond to $P4/ncc$ but not $I4/mcm$ symmetry, with no apparent vanadium disorder.¹⁶ The differences in space group symmetry and vanadium ordering, and the significant difference between the reported and our own values of c , suggest that moderate pressure results in a vanadyl ordered (α) form of $\text{VO}(\text{H}_2\text{AsO}_4)_2$, whereas preparations at atmospheric pressure result in the disordered (β) modification.

(15) Amoros, P.; Beltran-Porter, A.; Beltran-Porter, D.; Villeneuve, G. *Eur. J. Solid State Inorg. Chem.*, in press.

(16) Wang, S. L.; Lee, W. C. *Acta Crystallogr.* 1991, C47, 1709.

Table III. Final Profile and Structural Parameters for $\text{Li}_4\text{VO}(\text{AsO}_4)_2$ in Space Group $P4/ncc$ (No. 130), with Esd's in Parentheses

Cell Dimensions (Å)						
		$a = 9.0293$ (2)			$c = 9.0053$ (4)	
Data						
no. of reflns = 557		no. of points = 3533		no. of refined params = 32		
$R_{wp} = 13.8$		R Factors (%) $R_p = 10.4$		$R_F = 9.3$		
Atomic Parameters						
atom	sym position	x	y	z	isotrop B-factor, Å ²	site occ
V(1)	4c	1/4	1/4	0.213 (1)	1.8 (3)	0.65 (1)
V(2)	4c	1/4	1/4	0.341 (2)	1.8	0.35
As	8f	-0.0530 (2)	0.0530	1/4	0.81 (5)	1.0
O(1)	16g	0.1363 (9)	0.0742 (9)	0.277 (1)	1.2 (3)	1.0
O(2)	16g	0.873 (2)	0.120 (2)	0.0949 (9)	2.6 (3)	1.0
O(3)	4c	1/4	1/4	0.026 (1)	3.6 (7)	1.0
Li	16g	0.116 (2)	-0.167 (2)	0.104 (1)	7 (2)	1.0

Table IV. Selected Bond Distances (Å) and Angles (deg) for $\text{Li}_4\text{VO}(\text{AsO}_4)_2$, with Esd's in Parentheses

V(1)-O(1) (×4)	1.976 (9)	As-O(2) (×2)	1.662 (8)
V(1)-O(3)	1.69 (1)	Li-O(1)	2.05 (1)
V(1)-O(3)'	2.82 (1)	Li-O(1)'	2.69 (2)
V(2)-O(1) (×4)	1.976 (9)	Li-O(2)	1.84 (1)
V(2)-O(3)	1.66 (1)	Li-O(2)'	1.86 (1)
V(2)-O(3)'	2.84 (1)	Li-O(2)''	2.42 (2)
As-O(1) (×2)	1.737 (8)		
O(1)-V(1)-O(1)	85.1 (2)	O(1)-V(2)-O(3)'	73.0 (5)
O(1)-V(1)-O(1)'	146.1 (7)	O(3)-V(2)-O(3)'	180
O(1)-V(1)-O(3)	107.0 (4)	O(1)-As-O(1)'	103.8 (6)
O(1)-V(1)-O(3)'	73.0 (4)	O(1)-As-O(2)	101.1 (6)
O(3)-V(1)-O(3)'	180	O(1)-As-O(2)'	118.3 (6)
O(1)-V(2)-O(1)	85.1 (3)	O(2)-As-O(2)'	114.5 (6)
O(1)-V(2)-O(1)'	146 (1)	V(1)-O(1)-As	124.0 (5)
O(1)-V(2)-O(3)	107.0 (5)	V(2)-O(1)-As	129.9 (5)

The structure of $\text{Li}_4\text{VO}(\text{AsO}_4)_2$ (Figure 5) is very similar to that of the parent compound, showing that the ion-exchange reaction occurs topotactically, as might be expected under the "chimie douce" conditions used. This is accompanied by an 11% expansion in the *c*-direction, due to the insertion of Li^+ ions close to the intersection of the interlamellar spaces and the channels parallel to *c*. The restrained refinement of the lithium position shows it to be in an irregular, five-coordinate site, with Li-O distances varying between 1.84 and 2.69 Å. Chemical analysis of this material previously gave the stoichiometry $\text{Li}_4\text{VO}(\text{AsO}_4)_2 \cdot 0.5\text{H}_2\text{O}$,⁹ but whether the water is disordered within the structure or is present in an amorphous phase is not clear. A powder neutron study will be performed to resolve this matter and obtain a more accurate refinement of the lithium position.

Refining the structure of $\text{Li}_4\text{VO}(\text{AsO}_4)_2$ in space group $P4/ncc$ allows the two V sites within the VO_6 octahedra to be varied, giving occupation factors of 0.65 and 0.35. The results in Table IV show that the two sites have similar coordination geometries, with the vanadiums displaced from the center of an axially elongated octahedron. Both the mean V=O bond length of 1.68 Å and especially the mean V...O distance of 2.83 Å are greater than the corresponding distances of 1.61 and 2.46 Å in $\text{VO}(\text{H}_2\text{AsO}_4)_2$, due to the increased interlayer separation.

Infinite $\cdot\text{V}=\text{O}\cdots\text{V}=\text{O}\cdot$ chains have been found in a variety of oxo salts in which the V atom is displaced from the center of an octahedron toward one of the two apically-shared oxygens (see Table V).^{10,17-23} Disorder of the vanadium atom is evidenced in

Table V. Vanadium-Oxygen Distances (Å) and Site Occupation Factors for Oxo Salts Containing Infinite (Exception: *e*) Vanadyl Chains

compd	distance, Å ^a		site occ factors		ref
	V=O	V...O	V	V'	
$\alpha\text{-VO}(\text{SO}_4)$	1.63	2.47	1.0		17
$\text{VO}(\text{MoO}_4)$	1.68	2.59	1.0		18
$\text{VO}(\text{H}_2\text{PO}_4)_2$	1.60	2.38	1.0		10
$\text{Zn}_2\text{VO}(\text{PO}_4)_2$	1.57	2.95	1.0 ^b	<i>c</i>	19
$\text{VOSi}(\text{PO}_4)_2$	1.59	2.49	1.0		20
$\alpha\text{-VO}(\text{H}_2\text{AsO}_4)_2$	1.60	2.48	1.0		16
$\beta\text{-VO}(\text{H}_2\text{AsO}_4)_2$	1.61	2.46	0.50	0.50	this work
$\text{Li}_4\text{VO}(\text{AsO}_4)_2$	1.68	2.83	0.65	0.35	this work
$\text{VO}(\text{HPO}_4) \cdot 0.5\text{H}_2\text{O}$	1.57	2.35	1.0		21
$(\text{VO})_2\text{P}_2\text{O}_7$	1.73	2.21	1.0 ^b		22
	1.70	2.16	1.0 ^b		
	1.53	2.34	1.0		
	1.55	2.37	1.0		
$\text{Rb}(\text{VO})_3(\text{P}_2\text{O}_7)_2\text{O}_{0.14}$	1.82	1.82	1.0 ^{b,d}		23
	1.59	2.49	0.54 ^e	0.46 ^e	

^aThe distances are a weighted average of those for the V and V' sites, which are displaced in opposite directions from the center of the VO_6 octahedra in the chain direction. ^bA large anisotropic thermal parameter was reported for V parallel to the chain direction. ^cA peak in the final Fourier difference map was observed close to the V' position. ^dV and V' sites are coincident. ^eThis site is part of a linear chain of four vanadyl groups.

many of these refinements by large anisotropic thermal parameters in the chain direction, elongation of the V=O and shortening of the V...O distances, residual electron density at the alternative V site, and split site refinements of the V atom. The correlation between disorder and apparent V-O distances is especially notable when comparing the four independent chains in $(\text{VO})_2\text{P}_2\text{O}_7$.²¹ The values of V-O distances in such disordered chains should thus be treated with suspicion if they are to be related to other properties such as vibrational or electronic absorption frequencies.

This disorder cannot satisfactorily be described as arising from random displacements of V atoms within each chain, as this would result in many energetically unfavorable $\text{V}=\text{O}=\text{V}$ and $\text{V}\cdots\text{O}\cdots\text{V}$ groups. Instead, we propose that all of the V displacements within each chain are parallel, giving rise to well-ordered vanadyl chains that may be described by a single "chain displacement" (+ or - along the chain direction), but that the displacements of neighboring chains are partially or, in the case of $\beta\text{-VO}(\text{H}_2\text{AsO}_4)_2$, completely uncorrelated. Evidence for highly developed intrachain ordering in $\beta\text{-VO}(\text{H}_2\text{AsO}_4)_2$ comes from the ease in changing the layer separation during the Li exchange reaction; this requires a regular alternation of strong and weak V-O bonds perpendicular to the layers.

(17) Longo, J. M.; Arnott, R. J. *J. Solid State Chem.* **1970**, *1*, 394.(18) Eick, H. A.; Kihlberg, L. *Acta Chem. Scand.* **1966**, *20*, 722.(19) Lii, K. H.; Tsai, H. J. *J. Solid State Chem.* **1991**, *90*, 291.(20) Middlemiss, N.; Calvo, C. *Acta Crystallogr.* **1976**, *B32*, 2896.(21) Leonowicz, M. E.; Johnson, J. W.; Brody, J. F.; Shannon, H.; Newsam, J. M. *J. Solid State Chem.* **1985**, *56*, 370.(22) Gorbunova, Y. E.; Linde, S. A. *Dokl. Akad. Nauk SSSR* **1979**, *245*, 584.(23) Lii, K. H.; Lee, C. S. *Inorg. Chem.* **1990**, *29*, 3298.

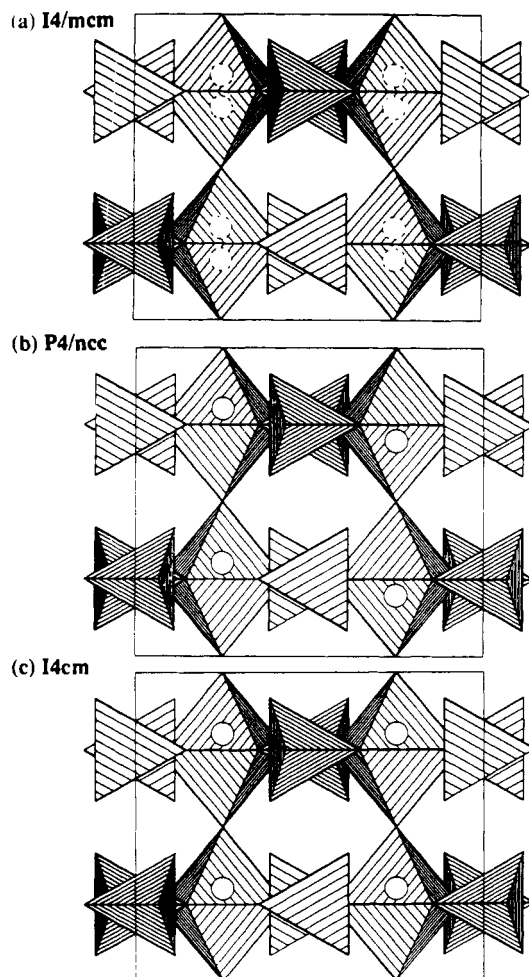


Figure 6. (010) polyhedral view (c vertical) of idealized $\text{VO}(\text{XO}_4)_2^{4-}$ layers showing (a) disorder, (b) antiparallel order, and (c) parallel order of the vanadium displacements in neighboring chains with the resulting space group symmetries marked.

Interchain ordering of the V displacements results from direct electrostatic dipolar interactions, which favor an antiparallel alignment of neighboring chains, and through the resultant displacements of oxoanions linking the chains. In a comparison of the structures of $\text{VO}(\text{H}_2\text{PO}_4)_2$ and $\beta\text{-VO}(\text{H}_2\text{AsO}_4)_2$, the latter mechanism seems to be the more important, as the distances between chains (6.33 and 6.45 Å, respectively) do not differ greatly. Hence, the fact that the chain displacements are strongly

correlated in $\text{VO}(\text{H}_2\text{PO}_4)_2$ but are completely randomized in $\beta\text{-VO}(\text{H}_2\text{AsO}_4)_2$ may be directly attributed to the difference between the rigid phosphate groups and more flexible arsenate groups that connect each vanadyl chain to four neighboring chains. The flexibility of the arsenate group also enables a facile Li^+ exchange reaction to occur in $\beta\text{-VO}(\text{H}_2\text{AsO}_4)_2$ that is not observed in $\text{VO}(\text{H}_2\text{PO}_4)_2$, which induces a slight interchain ordering of the vanadyl displacements. These results suggest that vanadyl arsenates should display a richer ion exchange and intercalation chemistry than analogous phosphates.

For the $\text{VO}(\text{XO}_4)_2^{4-}$ derivatives ($\text{X} = \text{P}, \text{As}$), ordering of the chain displacements reduces the symmetry from $I4/mcm$ in the completely disordered case (Figure 6a) to either $P4/ncc$, with antiparallel displacements (Figure 6b), or $I4cm$, with parallel displacements (Figure 6c). Both types of order have been observed; $\text{VO}(\text{H}_2\text{PO}_4)_2$,¹⁰ $\alpha\text{-VO}(\text{H}_2\text{AsO}_4)_2$,¹⁶ and $\text{Li}_4\text{VO}(\text{AsO}_4)_2$ have $P4/ncc$ symmetry whereas $\text{Zn}_2\text{VO}(\text{PO}_4)_2$ ¹⁹ has $I4cm$ symmetry. In all of these structures the additional cations occupy approximately the same position, although in the protonated compounds the hydrogen is displaced toward one of the oxygens. This suggests that the adopted structure is controlled by the number of cations, as the four available cation sites remain equivalent in $P4/ncc$ symmetry but are split into two pairs in $I4cm$. Thus, the former symmetry prevails when four monovalent cations are present, but the latter is favored for two divalent cations and two vacancies. $\text{VO}(\text{Si}(\text{PO}_4)_2)$ ²⁰ and the isostructural $\text{MoOAl}(\text{PO}_4)_2$ ²⁴ also have $P4/ncc$ symmetry, as this allows the phosphate groups to rotate and provide tetrahedral coordination to the silicon or aluminum atom in the center of the channel at $(\frac{1}{4}, \frac{3}{4}, 0)$.

It is interesting to note that the $P4/ncc$ $\text{VO}(\text{XO}_4)_2^{4-}$ structure is closely related to that of Bi_2CuO_4 ,^{25,26} which has the same space group symmetry, and is shown in Figure 3b. In the latter $\text{M}(\text{XO}_2)_2$ structure ($\text{M} = \text{Cu}, \text{X} = \text{Bi}$) infinite stacks of MO_4 square planes are linked through O-X-O bridges. The addition of an oxygen between the M cations and of two more oxygens on each X atom gives the $\text{MO}(\text{XO}_4)_2^{4-}$ structure ($\text{M} = \text{V}, \text{X} = \text{P}, \text{As}$) with infinite chains of MO_6 octahedra connected through $\text{O-XO}_2\text{-O}$ linkages. The insertion of three anions into the closely packed Bi_2CuO_4 structure results in a more open arrangement into which cations can be introduced.

Acknowledgment. We acknowledge the British Council and Ministerio de Educacion y Ciencia (Spain) for funding from the Acciones Integradas Programme. M.A.G.A. thanks the Spanish Government for a Studentship.

- (24) Leclaire, A.; Borel, M.; Grandin, A.; Raveau, B. *Z. Krist.* **1990**, *190*, 135.
 (25) Boivin, J. C.; Thomas, D.; Tridot, G. *C. R. Acad. Sci. Paris C* **1973**, *276*, 1105.
 (26) Atfield, J. P. *J. Phys.: Condens. Matter* **1989**, *1*, 7045.